PAPER

Effective Echo Detection and Accurate Orbit Estimation Algorithms for Space Debris Radar

Kentaro ISODA[†], *Student Member*, **Takuya SAKAMOTO**[†a)], *Member*, **and Toru SATO**[†], *Fellow*

SUMMARY Orbit estimation of space debris, objects of no inherent value orbiting the earth, is a task that is important for avoiding collisions with spacecraft. The Kamisaibara Spaceguard Center radar system was built in 2004 as the first radar facility in Japan devoted to the observation of space debris. In order to detect the smaller debris, coherent integration is effective in improving SNR (Signal-to-Noise Ratio). However, it is difficult to apply coherent integration to real data because the motions of the targets are unknown. An effective algorithm is proposed for echo detection and orbit estimation of the faint echoes from space debris. The characteristics of the evaluation function are utilized by the algorithm. Experiments show the proposed algorithm improves SNR by 8.32 dB and enables estimation of orbital parameters accurately to allow for re-tracking with a single radar.
key words: space debris, KSGC radar, orbit estimation, coherent integration

1. Introduction

Space debris, such as fragments of satellites and rocket bodies orbiting the earth, is regarded as an environmental problem. More than 2,000 tons of artificial objects are in the earth's orbit, and 95% of these items are not functioning. In the event of the circular motion at the altitude of 500 km, the average relative velocity of space debris is about 10 km/s. As kinetic energy is proportional to the square of the velocity, the collision energy is enormous, and thus even tiny debris may cause serious damage to spacecraft.

The number of space debris with a diameter larger than 10^{-3} m is greater than 3.5 million [1], [2]. Therefore, the possibility that space debris could collide with operational spacecraft is likely. For these reasons, obtaining precise orbital information by observing space debris is indispensable for avoiding accidents. Space debris with a size greater than 0.1 m has been observed and cataloged with a network of multiple radars and optical sensors by US SPACECOM in the United States [3].

The KSGC (Kamisaibara Spaceguard Center) radar system was built by the Japan Space Forum as the first radar facility in Japan devoted to the observation of space debris and began operations in 2004. Table 1 shows the main parameters of the KSGC radar. The KSGC radar is equipped with an active phased array antenna mounted on a rotational base. Therefore, it is possible to track unknown targets for the full angular region above a 15 degree elevation such that

Table 1 Main parameters of the KSGC radar.

Parameters	Value
Location	Kamisaibara, Okayama, Japan (35.31°N, 133.94°E)
Radar System	Active Phased Array
Antenna Size	2.8 m × 2.8 m
Number of Elements	1,395
Antenna Gain	38.4 dB
Peak Output	96 kW (69 W × 1,395)
Polarization	Vertical
Center Frequency	3,265 MHz
Beam Width	1.9°
Range Resolution	225 m
Band Width	800 kHz
Pulse Length	200 or 300 μsec

the orbit can be determined by a single observation pass. Moreover, it has the ability to simultaneously observe ten pieces of debris with the time division control.

When considering the danger of collisions with spacecraft, only debris larger than 0.01 m needs to be observed as fragments smaller than 0.01 m do not damage spacecraft with surface protection materials. Currently, the KSGC radar system can observe space debris with a RCS (Radar Cross-Section) larger than 1 m^2 for a range of 600 km. In the future, the radar system will be used to observe 0.01 m debris. Effective algorithms for echo detection and orbit estimation of the faint echoes from space debris [4] are proposed as follows.

2. Conventional Method Utilizing Incoherent Integration

Linear-chirp pulse compression is used for the KSGC radar system to enhance the range resolution and SNR. We define $s_t(t) \exp(-j2\pi f_c t)$ as the transmitted signal, and $s_r(t)$ as the received signal after synchronous detection. They are expressed as

$$s_t(t) = A(t) \exp\left(-j2\pi \frac{B}{2T} t^2\right), \tag{1}$$

$$s_r(t) = s_t(t - t_d) \exp\left[-j2\pi \{f_d(t - t_d) - f_c t_d\}\right], \tag{2}$$

where $A(t)$, T, B, t_d, f_d, f_c are the window function, the pulse length, the frequency bandwidth, the delay time, the Doppler frequency, and the center frequency, respectively. This is applied to the matched filter whose impulse response is expressed as

$$h'(t) = s_t^*(-t), \tag{3}$$

where * means a complex conjugate, and estimate the delay time. The pulse compression ratio R_{pc} is expressed by $R_{pc} = BT$. The range resolution is improved by R_{pc}, and the peak output power is also enhanced by R_{pc} [5].

However, the delay time includes an error if the Doppler frequency has an offset. Figure 1 shows a model of the linear-chirp pulse compression. Solid lines of $s_t(t)$ and $s_r(t)$ are the transmitted and received signal, respectively. $s_r(t)$ has a time offset t_d and a frequency offset f_d as in this figure. $h(t)$ has a frequency offset f_d compared to $h'(t)$, that is matched to $s_r(t)$. We convolute $s_r(t)$ with the matched filter without the effect of the Doppler shift $h'(t)$ and obtain the delay time including the error of t_e, which is expressed as $t_e = f_d T/B$. The Doppler shift has to be considered for the matched filter, which is expressed as $h(t) = h'(t)\exp(-j2\pi f_d t)$. Therefore, there is ambiguity between the delay time and the Doppler frequency.

If f_d is accurate, an accurate delay time can be obtained where the response of the filter is at maximum. In an echo detection method using a single pulse, we search for the Doppler frequency which maximizes the response of the matched filter as

$$\max_{f_d, t} \left| \int s_r(\tau) h(t - \tau) d\tau \right|^2 . \tag{4}$$

In order to detect echoes, incoherent integration is effective to reduce fluctuation of signal due to noise. Incoherent integration does not require adjustment of phases and is thus easy to implement. We define N as the number of integrations and call each pulse a 'hit.' The SNR is not ameliorated, but noise fluctuation is reduced to $1/\sqrt{N}$ with incoherent integration, which makes it easy to detect echoes. Equation (4) is expanded to incoherent integration as

$$\max_{v_d, t} \sum_{i=1}^{N} \left| \int s_{ri}(\tau) h_i(t - 2iv_d T_{IPP}/c - \tau) d\tau \right|^2 , \tag{5}$$

where $s_{ri}(t)$ is the received signal for i-th pulse, $h_i(t)$ is the impulse response with the Doppler shift, T_{IPP} is IPP (Inter Pulse Period), and c is the velocity of light, $v_d = f_d c/2f_c$ is Doppler velocity respectively. In observation of space debris, the range changes by $2v_d NT_{IPP}$ in the integration duration. If we set $v_d = 4 \, \text{km/sec}$, $N = 16$, $T_{IPP} = 7,500 \, \mu\text{sec}$, $2v_d NT_{IPP}$ becomes 960 m, which is longer than the range resolution $\Delta r = 225$ m. Therefore, the time shift $2iv_d T_{IPP}/c$ is utilized in Eq. (5). In this paper this method is termed the incoherent method.

Figure 2 shows the result of the incoherent method applied to the real data of the KSGC radar. The left and right figures are echoes from H2A-R/B (H2A-Rocket Booster) and LCS-4 (The Lincoln Calibration Sphere) [6] whose RCS are 27.6 m^2 and 1 m^2, respectively. Figure 2 shows the difficulty in detecting echoes in low SNR condition even if incoherent integration is used. Therefore, in order to detect the faint echoes, it is necessary to develop a method to improve the SNR.
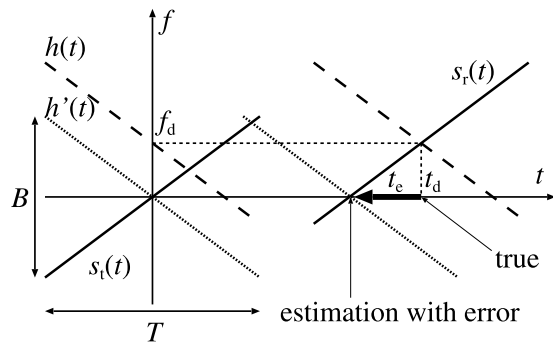

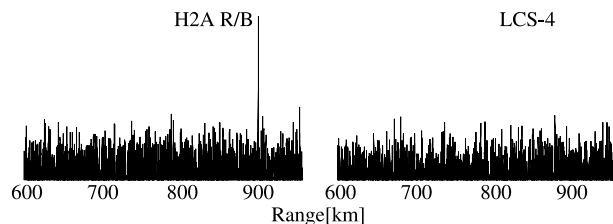
Fig. 1   Linear-chirp pulse compression.

Fig. 2   Example of the incoherent method applied to the real data.

3. Coherent Integration Utilizing a Motion Model

In order to improve SNR, we integrate received signals coherently. The range, the Doppler frequency, and the phase of signals from space debris change at every pulse during observation. Therefore, the parameters have to be updated for each pulse. However, coherent integration is difficult to calculate as the motion of space debris is unknown.

The instantaneous orbit of space debris is an ellipse with a focus at the center of earth's gravity. The orbit can be approximated as a uniform motion within a short time. We approximate an orbit of space debris as a uniform motion and take the coordinate plane including the orbit and the radar antenna. Figure 3 shows the system model. The orbit can be expressed with 3 parameters $(r_1, v_{d1}, \phi_1) = \boldsymbol{x}$. The range, the Doppler frequency, and the phase of space debris are expressed as

$$r_d(t) = \sqrt{r_1^2 - 2r_1 v_{d1} t + \left(\frac{v_{d1}}{\cos \phi_1} \right)^2 t^2}, \tag{6}$$

$$f_d(t) = -\frac{2f_c}{c} \frac{dr_d(t)}{dt}, \tag{7}$$

$$\theta(t) = -\frac{4\pi r_d(t)}{c} f_c, \tag{8}$$

where r_1, v_{d1} and ϕ_1 are the range, the Doppler velocity, and the angle between the direction of the motion and the line-of-sight of the first echo, respectively. The received signals are integrated coherently according to Eqs. (6), (7), and (8), and the evaluation function

$$E(\boldsymbol{x}) = \left| \sum_{i=1}^{N} \int s_{ri}(\tau) h_i(t_{di} - \tau) d\tau \cdot \exp(j\Delta\theta_i) \right|^2 \tag{9}$$
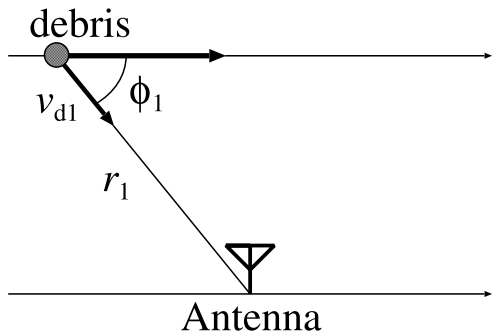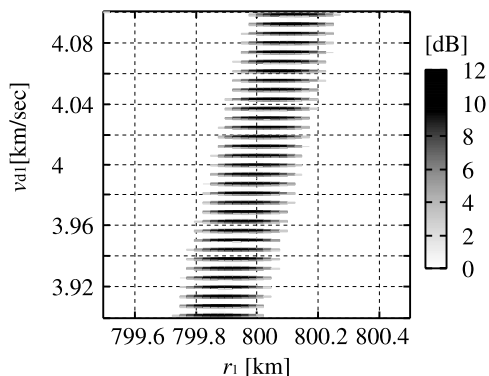
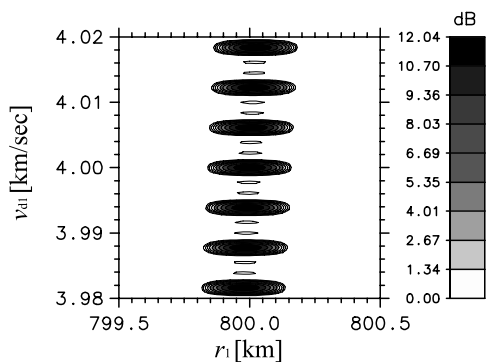**Fig. 3** System model.

Fig. 4 Evaluation function for true ϕ_1.

Fig. 5 Evaluation function for true ϕ_1 in detail.

Fig. 6 Evaluation function for true v_{d1}.

Fig. 7 Evaluation function for true r_1.

tion function for true ϕ_1, v_{d1}, and r_1 respectively, where $x = (800\,\text{km}, 4\,\text{km/s}, 60\circ)$, $N = 4$, $T_{IPP} = 7,500\,\mu\text{sec}$, and pulse length $T = 300\,\mu\text{sec}$. Figure 5 is a part of Fig. 4. These figures have the following two significant characteristics: First, the correlation between r_1 and v_{d1} is shown in Fig. 4. As explained in Sect. 2, the ambiguity between the delay time and the Doppler frequency caused by the linear-chirp pulse compression and its gradient α is expressed as

$$\alpha = \frac{B}{f_c T}. \tag{12}$$

This equation shows the gradient of the correlation is uniquely determined by the parameters of the radar systems. Second, there are many periodic peaks in the direction of v_{d1} in Figs. 5 and 7. This is due to the occurrence of cycle-slip when determining the Doppler velocity. Figure 8 shows the model of a uniform motion in a line-of-sight. In this case, the range changes by $v_d T_{IPP}$ at every pulse, which also changes the phase of each pulse. If the error corresponds to half the wavelength $\lambda/2$, coherent integration can be applied, where λ is the carrier wavelength. Therefore, many suboptimal solutions are generated in the direction of v_{d1}. We define v_{d0} as this period, which is expressed as

$$v_{d0} \simeq \frac{\lambda}{2T_{IPP}}. \tag{13}$$

v_{d1} has to be searched for in the accuracy of m/s as it is un-

is maximized, where t_{di} is the delay time for i-th pulse, and $\Delta\theta_i(i = 1, \cdots, N)$ is the difference of a phase between the first pulse and the i-th pulse. They are uniquely determined with $x = (r_1, v_{d1}, \phi_1)$. There are expressed as

$$t_{di} = 2r_d((i-1)T_{IPP})/c \tag{10}$$
$$\Delta\theta_i = 2\pi f_c(t_{d1} - t_{di}) \tag{11}$$

In Eq. (9), we convolute $s_{ri}(t)$ and $h_i(t)$, and find the optimum the delay time, the Doppler frequency, and the phase to maximize $E(x)$. Coherent integration is then applied. In order to estimate an orbit we search for x which maximizes the power after coherent integration. The orbit estimation process can be regarded as an optimization problem.

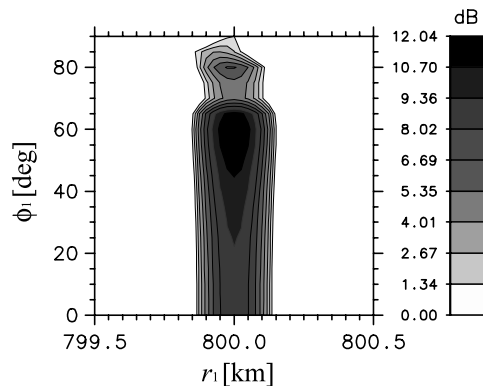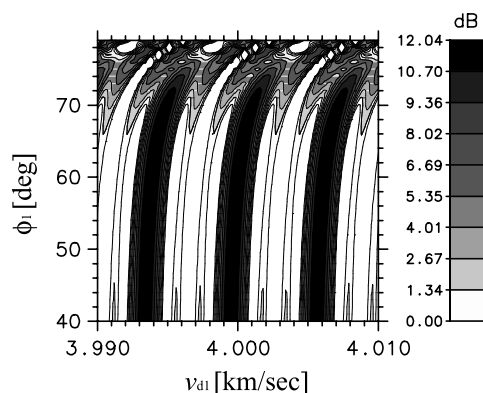Figures 4, 5, 6, and 7 show a part of the evalua-

Fig. 8 Ambiguity in determining v_{d1}.

Table 2 Comparison of the detection algorithms.

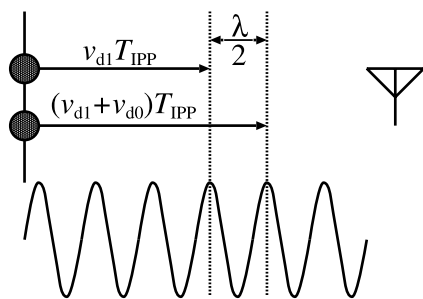|	$\Delta\theta_i$	t_{di}	$h_i(t)$
conventional	update	update	update
proposed	update	fixed	fixed

realistic to use the units of typical parameters of the KSGC radar which are $\lambda = 0.0918$ m and $T_{IPP} = 10$ ms. It is difficult to find a global solution because of these reasons. Therefore, an effective optimization method needs to be developed. Here, the optimization algorithm is divided into two stages; echo detection and orbit estimation.

4. Effective Echo Detection Algorithm

4.1 Proposed Detection Algorithm

An echo detection method is proposed in this section. The proposed algorithm detects the desired echoes, where the orbital parameters are disregarded. One of the suboptimal solutions in this algorithm is effectively found. Table 2 shows the comparison of the detection algorithms.

To find a suboptimal solution the correlation between r_1 and v_{d1} is utilized. Figure 9 shows the outline of the proposed detection method. We define u-axis and w-axis as the orthogonal axis and the parallel axis to the direction of the correlation, respectively. The simplest method is a search with the parameters of u, v_{d1}, and ϕ_1 iteratively calculating the evaluation function. However, this method requires a long calculation time as a filtering process is necessary to update the parameters.

In order to decrease the calculation time, the calculation of the evaluation value is simplified. The local shape of the evaluation function is especially dependent on the phase difference $\Delta\theta_i$ when compared to the other factors. According to Eq. (13), the Doppler velocity is divided into nv_{d0} and δv_d. They are expressed as

$$v_d = nv_{d0} + \delta v_d, \tag{14}$$

where n is an integer and $|\delta v_d| < v_{d0}/2$. We define nv_{d0} and δv_d as the global Doppler velocity and the local Doppler velocity, respectively. The global Doppler velocity determines the orbit of debris and influences the response of the matched filter. The local Doppler velocity determines the phase difference. Updating nv_{d0} requires a long calculation time due to the filtering process. In order to omit the filtering process we approximate $nv_{d0} + \delta v_d$ as nv_{d0} except for Eq. (11).

Figure 10 shows a section of the evaluation function in the direction of the v_{d1} axis. In this figure, the dashed

line corresponds to the true evaluation function. The solid line is the section of the simplified evaluation function using δv_d instead of v_{d1}. As v_{d1} shifts from the true value $v_{d1} = 4$ km/s, the evaluation values of the peaks become small due to the error of the Doppler frequency. On the other hand, in the case of δv_d, the evaluation values of the peaks are constant because other parameters are fixed. If δv_d is less than v_{d0}, we can approximate v_{d1} as δv_d. In the simplified evaluation function, the Doppler frequency for the matched filter is fixed. Therefore, pulse compression process is not required when searching along δv_d axis. This characteristic can be applied for ϕ_1, which is utilized to develop a high-speed algorithm.

We define x_{exp}, W_{th}, Δu, Δv_d, and $\Delta\phi$ as an expected orbital parameter, a threshold, and step widths of u, δv_d and $\delta\phi$, respectively. Δu corresponds to the projected amount of the range resolution and Δr to u axis, which is expressed as $\Delta u = \alpha\Delta r$. Δv_d and $\Delta\phi$ are a -3 dB width of v_{d1} and ϕ_1 in the evaluation function. The echo detection algorithm is described as follows:

1. Set the search area with x_{exp}. $k \leftarrow 1$. $x \leftarrow x_{exp}$.
2. If k is an odd number, go to 3. Otherwise go to 4.
3. Update x by $\frac{\Delta u}{2}\frac{k-1}{2}$ in the direction of $-u$ axis from x_{exp}. Go to 5.
4. Update x by $\frac{\Delta u}{2}\frac{k}{2}$ in the direction of $+u$ axis from x_{exp}. Go to 5.
5. Search along δv_d and $\delta\phi$ axes with step widths of $\Delta v_d/2$ and $\Delta\phi/2$, and set E_{max} as the maximum evaluation value.
6. If $E_{max} > W_{th}$, go to 7. Otherwise $k \leftarrow k + 1$ and go to 2.
7. Optimize r_1 with the quasi-Newton's method. Detection.

Next, the calculation time of the proposed echo detection method is explained. We define T_c as the time to calculate an evaluation value. The calculation time is IKT_c to search along v_{d1} and ϕ_1 axes by I and K points. The calculation time of the proposed method is approximately T_c because the search along v_{d1} and ϕ_1 axes can be replaced by a simple phase rotation. The filtering process is not required when searching along v_{d1} and ϕ_1 axes. Therefore, the calculation time improves by IK. We search along v_{d1} axis with the step width of $\Delta v_d/2$. The number of calculations is expressed as $I = 2v_{d0}/\Delta v_d$. $K = 30$ is set as the number of calculations along the ϕ_1 axis. In this case, Δv_d and v_{d0} are 0.00034 km/s and 0.00612 km/s, respectively, where $N = 16$ and $T_{IPP} = 7,500$ μsec. Therefore, IK becomes 1,080 and the calculation time becomes 1,080 times shorter compared to the conventional method.
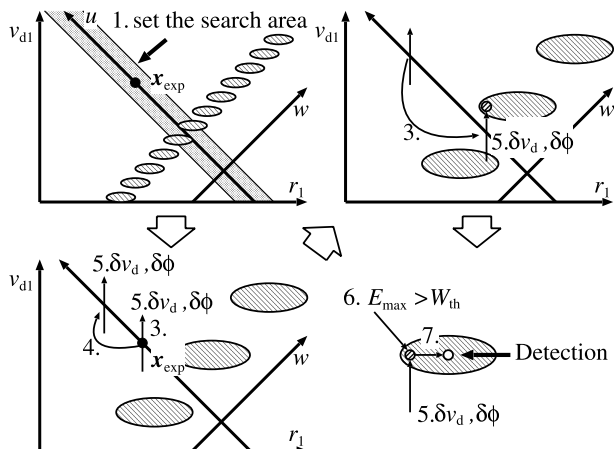
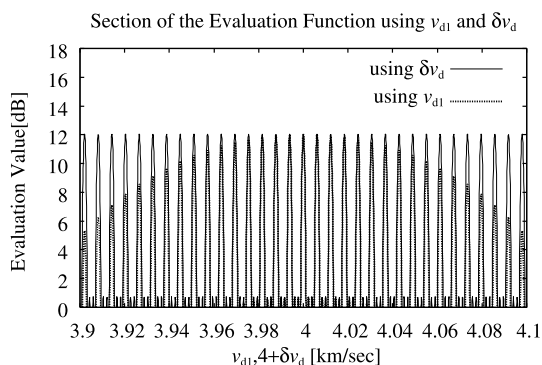**Fig. 9** Outline of the detection method.

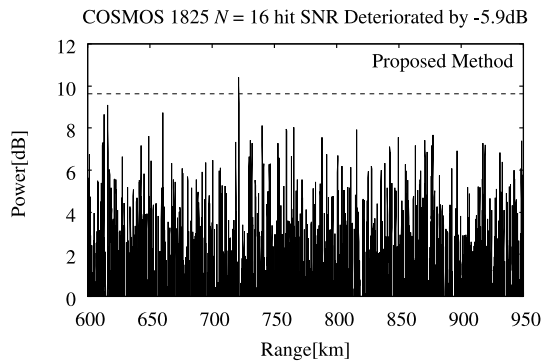**Fig. 10** Section of the evaluation function using v_{d1} and δv_d.

Fig. 11 Example of the proposed detection method applied to the real data.

Fig. 12 Example of the incoherent method applied to the real data.

4.2 Evaluation of the Proposed Echo Detection Method

As we explained in Sect. 1, the minimum detection size of the KSGC radar system is $1\,m^2$ for the range of $600\,km$. In order to clarify the improvement of the proposed detection method, noise was added to the real data to intentionally deteriorate SNR to simulate severe conditions.

Data from satellite COSMOS-1825 with RCS of $7.87\,m^2$ was used. The expected value is $x_{\exp} = (721.709\,km, -3.661\,km/s, 61.92°)$. According to the radar equation [7], the received power from the target with RCS $= 1\,m^2$ for the range of $600\,km$ is equivalent to the target whose RCS $= 2.085\,m^2$ for the range of $721\,km$. The received power of COSMOS-1825 is 3.77 times ($= 5.8\,dB$) larger than the minimum detection power. Gaussian noise was added to the real data to deteriorate SNR by $5.9\,dB$. In this case, the RCS corresponds to $2.0\,m^2$, which is the detection limit of the KSGC radar.

Figure 11 shows an example of the proposed detection method applied to the experimentally observed data of COSMOS-1825, where $N = 16$. Figure 12 shows an example of the incoherent method. The noise level is set to $0\,dB$ in these figures. In these figure, the value at the range determined by x corresponds to the evaluation value $E(x)$. Note
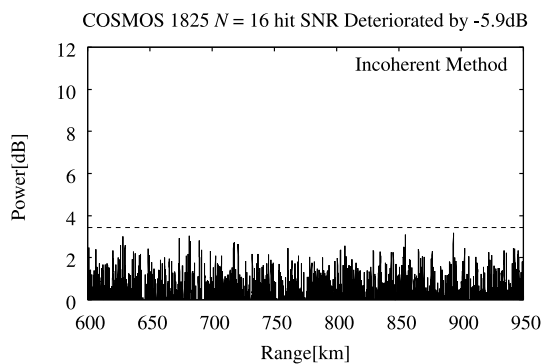
that the values in these figures are normalized by the noise level. The Doppler frequency used in the incoherent method is an expected value, that is used for the delay compensation and pulse compression for incoherent method, that has been explained in Sect. 2. Figure 12 is a close-up of these figures. The peak SNR is shown to improve by $8.0\,dB$ compared with the incoherent method. In this case, the effect of coherent integration is smaller than $12\,dB$ because the received power from space debris is not constant.

Next, the determination of the threshold is discussed. If a power larger than the threshold is detected, the desired echo is located. The threshold is determined with the false alarm probability. The method to keep the false alarm probability constant is called CFAR (Constant False Alarm Rate) [8]. The idea of CFAR is adopted for the detection of debris. P_{fa} is defined as the false alarm probability and is set as 10^{-4}. In this case, the thresholds of the proposed method and the incoherent method are $9.64\,dB$ and $3.43\,dB$, respectively, compared with the average noise level. The dashed lines in Figs. 11 and 12 are the thresholds. Figures 11 and 12 show that the proposed algorithm identifies the echo which cannot be detected by the conventional incoherent method.

We define x_{det} as the obtained parameters with the proposed detection method. In the case described above, we obtain $x_{det} = (721.416\,km, -3.274\,km/s, 62.92°)$ which causes the difference in range of the peak between the proposed detection method and the incoherent method in Fig. 13. The
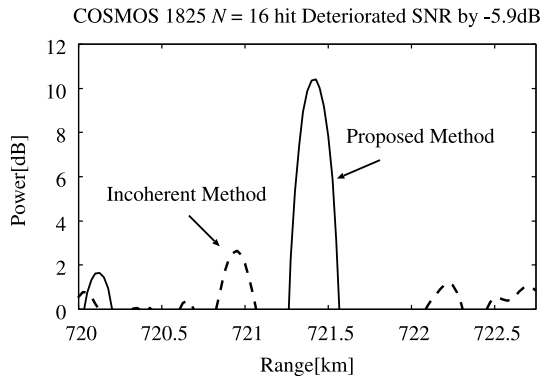
Fig. 13 Comparison between the proposed detection method and the incoherent method.

Fig. 14 Quasi-period problems.

Fig. 15 Outline of the estimation method.

estimated parameters with the echo detection algorithm has errors. Therefore, global optimization is required with these estimated parameters as the initial values to accurately estimate the orbital parameters.

5. Accurate Orbit Estimation Algorithm

An orbit estimation method is described in this section. The global optimal solution is searched for with the initial parameters x_{det} estimated from the echo detection algorithm of the previous section. It is difficult to globally optimize the evaluation function because it has many peaks along a diagonal line. We propose an effective algorithm to resolve this problem.

A simple strategy would be to update the parameters to increase the evaluation value with the linear search in the direction of w. However, this simple method is not accurate because the period varies slightly in the order of 10^{-3} m/s. This is due to the nonlinearity of the change in Doppler velocity as expressed in Eq. (7), which shows that the evaluation function has a quasi-periodicity. Equation (13) is accurately satisfied if the motion of space debris is uniform for line-of-sight. The dashed line in Fig. 14 displays the procedure of this simple method. The estimated points gradually shift from the local maxima. Therefore, this simple algorithm does not work for actual data.

In order to estimate accurate orbital parameters, x has to be updated to the next suboptimal solution according to v_{d0} in the direction of w. The evaluation function has to be optimized each time. The solid lines in Fig. 14 show the procedure of this method. As previously explained in Sect. 4.1, this method requires a long calculation time as filtering is needed for every update. A new orbit estimation algorithm is proposed which solves the problem of long calculation time.

In order to optimize x, we introduce δv_d and $\delta \phi$ similarly to the proposed echo detection method. In the local optimization, the fine parameters are optimized instead of the original parameters. Figure 15 illustrates the procedure of the proposed orbit estimation method. We define x_{est} as the orbital parameters obtained by the proposed orbit esti-
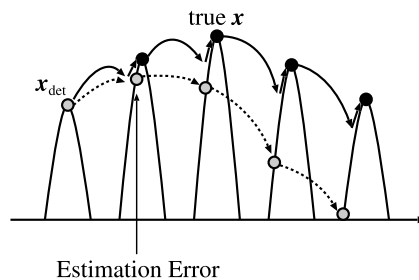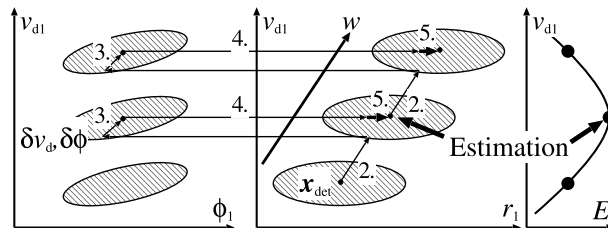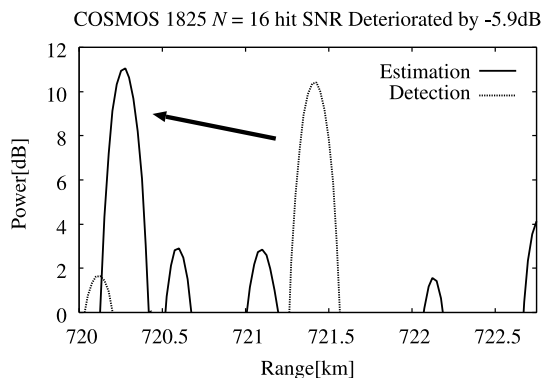

Fig. 16 Example of the proposed orbit estimation method applied to the real data.

mation method. The orbit estimation algorithm is described as follows:

1. $x \leftarrow x_{det}$.
2. $x \leftarrow x + (\alpha/v_{d0}, v_{d0}, 0)$.
3. Optimize $\delta v_d, \delta \phi$ with the quasi-Newton's method.
4. $x \leftarrow x + (0, \delta v_d, \delta \phi)$.
5. Optimize r_1 with the quasi-Newton's method, and set E as the evaluation value.
6. If E is the maximum value compared with the evaluation values of the previous steps. Go to 7. Otherwise go to 2.
7. $x_{est} \leftarrow x$.

Figure 16 shows the result of the proposed orbit estimation method applied to the experimental data in Fig. 11. The value at the range determined by x is normalized $E(x)$ just like as Figs. 11, 12. In this figure, the solid line is the coherently integrated signal with x_{est} and the dashed line is the same as the solid line in Fig. 13. The estimated range r_1 is updated by using the proposed orbit estimation algo-
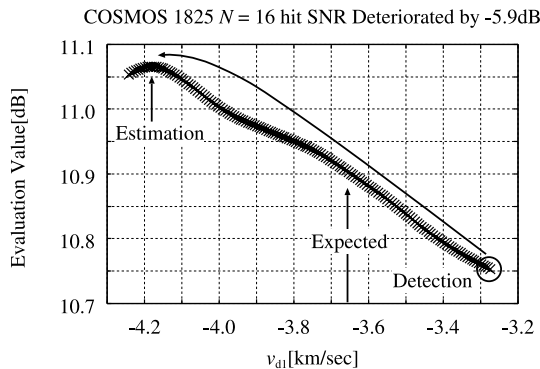
Fig. 17   Orbit estimation (v_{d1} section).

Table 3   Comparison of the detection, the orbit estimation, and the expected parameters.

	r_1 [km]	v_{d1} [km/s]	ϕ_1 [deg]
Detection x_{det}	721.422	−3.274	62.92
Estimation x_{est}	720.268	−4.180	57.16
Expected x_{exp}	721.709	−3.661	61.92
Erorr $\lvert x_{\text{est}} - x_{\text{exp}} \rvert$	1.44	0.519	4.76

rithm. Figure 17 shows the estimated orbit in the v_{d1} direction, which displays an evaluation value $E(x)$ in Eq. (9) is 0.32 dB higher than the detection method. Table 3 is the comparison between the detection, the orbit estimation, and the expected parameters, which shows the error of the estimated parameters are 1.44 km for r_1, 0.519 km/s for v_d and 4.76° for ϕ_1, respectively. Note that x_{exp} is not the true parameter but an expected parameter. In this case, x_{det} is accurate although this accuracy cannot be expected in general cases. In the next section, we evaluate the accuracy of the estimated parameters.

6.   Accuracy Evaluation with Experimental Data

The accuracy of the estimated parameters is examined in this section. Equation (5) is used to search for v_d which maximizes the response of the filter with incoherent integration. This method is simple as it does not require the signal phases. In this method, however, the error does not become zero even for the noiseless case because the motion of space debris is assumed to be uniform for line-of-sight.

Figures 18, 19, and 20 show the estimation errors vs. the peak SNR, where the true $x = (800\,\text{km}, 4\,\text{km/s}, 60°)$ and $N = 16$ is set. The estimation error is evaluated as RMSE (Root Mean Square Error). In this condition, the accuracy limit of the incoherent method is about 0.039 km/s for v_{d1}. These figures show the accuracy of the proposed method is better than the incoherent method for SNR ≤ 10 dB and 15 dB ≤ SNR. In the incoherent method, the estimation of r_1 has a large error for SNR of 0 dB because SNR is smaller than the detection limit.

To observe space debris larger than 0.01 m and determine the orbit, multiple large radar systems would be required around the world which is not realistic. Therefore,
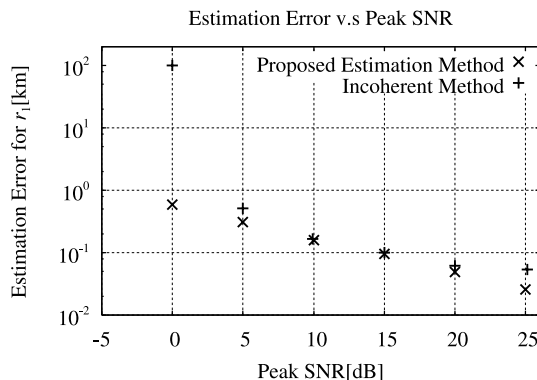

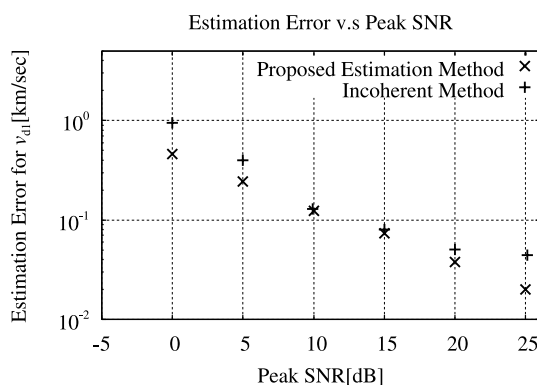**Fig. 18**   Accuracy of the proposed and incoherent methods for r_1.

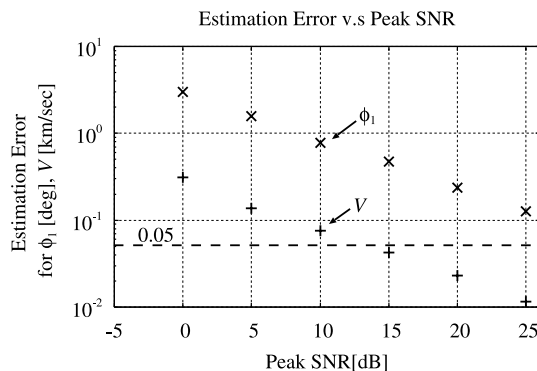**Fig. 19**   Accuracy of the proposed and the incoherent method for v_{d1}.

Fig. 20   Accuracy of the proposed and the incoherent method for ϕ_1.

the KSGC radar system is required to re-track space debris 24 hours later with the estimated position and the velocity obtained in a single observation pass. The velocity has to be estimated with an error smaller than 0.05 km/s for re-tracking. The velocity is expressed as $V = v_{d1} / \cos \phi_1$. The estimation error of V in Fig. 20 confirms that it is possible to re-track space debris 24 hours later for 13.6 dB ≤ SNR.

7.   Discussion

In order to obtain a velocity with an error less than 0.05 km/s, the estimated parameters with 16 pulses are av-

eraged over multiple CPI. CPI (Coherent Pulse Interval) is defined as a unit of the integration time, which shows that 16 hit = 1 CPI. The observation time in a single pass is about 5 minutes and the KSGC radar system can simultaneously observe 10 debris pieces. Therefore, the observation time for each debris is about 30 sec. The longest CPI is 160 msec in the case of the KSGC radar, and thus a piece of space debris can be observed for 187 CPI.

We define V_i as the estimated velocity for the i-th CPI and assume the variable V_i has white Gaussian errors with a standard deviation σ. The average $\overline{V} = \sum_{i=1}^{M} V_i/M$ follows $N(\mu, \sigma^2/M)$. The confidence interval of the confidence coefficient $1 - \gamma$ of μ is expressed as

$$\left[\overline{V} - \frac{\sigma}{\sqrt{M}}Z_{\gamma/2}, \overline{V} + \frac{\sigma}{\sqrt{M}}Z_{\gamma/2} \right], \tag{15}$$

where

$$Z_{\gamma/2} = \Phi^{-1}(1 - \gamma/2), \tag{16}$$

$$\Phi(z) = \int_{-\infty}^{z} \frac{1}{\sqrt{2\pi}}\exp\left(-z^2/2\right)\mathrm{d}z. \tag{17}$$

We define ε as the tolerance of V. The required average number for $\overline{V}$ to be satisfied with ε at the probability of $1 - \gamma$ is expressed as

$$M \geq \frac{\sigma^2 Z_{\gamma/2}^2}{\varepsilon^2}. \tag{18}$$

We define $M_{\max}$ as the maximum number of M. The limit of σ which can obtain the sufficient accuracy of V is expressed as

$$\sigma_{\lim} = \frac{\varepsilon\sqrt{M_{\max}}}{Z_{\gamma/2}}. \tag{19}$$

We assume $1 - \gamma = 0.99$, $\varepsilon = 0.05\,\text{km/s}$ and $M_{\max} = 187$ CPI. In this case $Z_{\gamma/2}$ is 2.576, and $\sigma_{\lim}$ is $0.2654\,\text{km/s}$, which corresponds to the peak SNR of $0\,\text{dB}$. This result shows that sufficient accuracy of the velocity can be obtained with the proposed method with a peak SNR greater than $0\,\text{dB}$.

In the observation of space debris, it is not realistic to continuously average the estimated parameters with a constant SNR because space debris changes position. According to the radar equation, SNR is inversely proportional to the 4-th power of the range. We define S_1 as SNR of the range r_1. The change of SNR is expressed as

$$S(t) = \left\{ \frac{r_1}{r_{\mathrm{d}}(t)} \right\}^4 S_1. \tag{20}$$

The square of the estimation error σ^2 is expressed as

$$\sigma^2(t) = 10^{2b}S^{20a}(t), \tag{21}$$

where $a = -0.055$ and $b = -0.545$, which are obtained by fitting V of Fig. 20 as a straight line, $\log\sigma = 10a\log\text{SNR} + b$. Here, σ is a function of SNR. a as $-1/20$ are approximated and replace 10^{2b} as C. We define T_{obs} and T_{CPI} as the
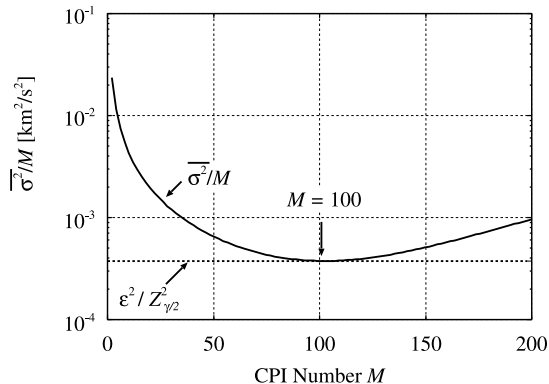

Fig. 21 The average number of CPI for re-tracking.

observation time and CPI, respectively. The mean value of σ^2 is expressed as

$$
\begin{aligned}
\overline{\sigma^2} &= \frac{C}{T_{\mathrm{obs}}} \int_0^{T_{\mathrm{obs}}} S^{-1}(t)\mathrm{d}t \\
&= \frac{C}{\zeta^2 S_1}\left(\frac{\chi^2}{5}T_{\mathrm{obs}}^4 + \frac{\xi\chi}{2}T_{\mathrm{obs}}^3 \right. \\
&\quad \left. + \frac{\zeta\chi + \xi^2}{3}T_{\mathrm{obs}}^2 + \zeta\chi T_{\mathrm{obs}} + \zeta^2 \right),
\end{aligned}
\tag{22}
$$

where $\zeta = r_1^2$, $\xi = -2r_1 v_{\mathrm{d}1}$, $\chi = (v_{\mathrm{d}1}/\cos\phi_1)^2$, $T_{\mathrm{obs}} = N_{\mathrm{d}}M T_{\mathrm{CPI}}$, N_{d} is the number of space debris pieces being observed. In order to estimate V with an error less than $0.05\,\text{km/s}$, the following condition should be satisfied.

$$\frac{\overline{\sigma^2}}{M} \leq \frac{\varepsilon^2}{Z_{\gamma/2}^2}. \tag{23}$$

Figure 21 illustrates M vs. $\overline{\sigma^2}/M$ for reference SNR $S_1 = 0.9\,\text{dB}$. The desired accuracy of the velocity is obtained when $\overline{\sigma^2}/M$ is less than the dashed line in Fig. 21. In order to estimate the limit condition $\overline{\sigma^2}/M$ touches with the dashed line because the estimation error has a minimum value.

8. Conclusion

We propose an echo detection method for the signals from space debris that cannot be identified with incoherent integration. The orbit of space debris is assumed to exhibit uniform motion in the proposed method. The calculation time for searching along the $v_{\mathrm{d}1}$ and ϕ_1 sections becomes about 1,080 times shorter in contrast to the simple method. The simple method uses a direct search for $v_{\mathrm{d}1}$ and ϕ_1, where the integration number is $N = 16$ and IPP is $7,500\,\mu\text{sec}$. The proposed detection method improves SNR by $8.0\,\text{dB}$ to the real data of the KSGC, derived from satellite COSMOS-1825, with applied Gaussian noise to deteriorate the SNR to the detection limit.

The proposed method estimates the orbit of space debris effectively with a high accuracy. The proposed orbit estimation method improves SNR by $0.32\,\text{dB}$ compared with

the proposed detection method. An example of the errors in the estimated parameters are 1.44 km for r_1, 0.519 km/s for v_{d1}, and 4.76 ° for ϕ_1, respectively. The estimation accuracy of the proposed orbit estimation method is greater than the incoherent method especially in a low SNR environment.

Our study confirms that if the orbital parameters and RCS are $x = (800\,\text{km}, 4.0\,\text{km}, 60°)$ and $0.36\,\text{m}^2$, sufficient accuracy of the velocity can be obtained with the proposed method.

Acknowledgment

References

[1] N.L. Johnson and D.S. McKnight, Artificial space debris, Orbit Book Co., p.111, 1987.

[2] National Research Council, Orbital debris, National Academy Press, p.210, 1995.

[3] P.A. Jackson, "Space surveillance satellite catalog maintenance," Orbital Debris Conference, Paper no.AIAA-1990-1339, April 1990.

[4] K. Isoda, T. Sakamoto, and T. Sato, "An effective orbit estimation algorithm for a space debris radar using the quasi-periodicity of the evaluation function," Proc. European Conference on Antennas & Propagation 2006, ESA SP-626, no.345431, Nov. 2006.

[5] M.I. Skolnik, Introduction to Radar Systems, Second ed., pp.422–427, McGraw-Hill, 1962.

[6] R.T. Prosser, "The Lincoln calibration sphere," Proc. IEEE, vol.53, pp.1672–1676, Oct. 1965.

[7] S.A. Hovanessian, Radar Detection and Tracking Systems, pp.1-4–1-6, Artech House, 1973.

[8] M.I. Skolnik, Radar Handbook, pp.5-29–5-31, McGraw-Hill, 1970.

Takuya Sakamoto was born in Nara, Japan in 1977. Dr. Sakamoto received his B.E. degree from Kyoto University in 2000, and M.I. and Ph.D. degrees from the Graduate School of Informatics, Kyoto University in 2002 and 2005, respectively. He is a research associate in the Department of Communications and Computer Engineering, Graduate School of Informatics, Kyoto University. His current research interest is in digital signal processing. He is a member of the IEEJ and the IEEE.

Toru Sato received his B.E., M.E., and Ph.D. degrees in electrical engineering from Kyoto University, Kyoto, Japan in 1976, 1978, and 1982, respectively. He has been with Kyoto University since 1983 and is currently a Professor in the Department of Communications and Computer Engineering, Graduate School of Informatics. His major research interests have been the system design and signal processing aspects of atmospheric radars, radar remote sensing of the atmosphere, observations of precipitation using radar and satellite signals, radar observation of space debris, and signal processing for subsurface radar signals. Dr. Sato was awarded the Tanakadate Prize in 1986. He is a member of the Society of Geomagnetism and Earth, Planetary and Space Sciences, the Japan Society for Aeronautical and Space Sciences, the Institute of Electrical and Electronics Engineers, and the American Meteorological Society.
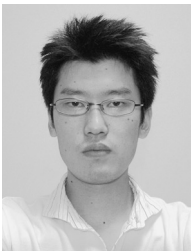
Kentaro Isoda was born in 1982. He received his B.E. degree from Kyoto University in 2005. He is currently studying for the M.I. degree at the Graduate School of Informatics, Kyoto University. His current research interest is in signal processing for space debris radar.